DOI: 10.13208/j.electrochem.200646
Cite this: *J. Electrochem.* **2020**, *26*(5): 740-749

Article ID:1006-3471(2020)05-0740-10
Http://electrochem.xmu.edu.cn

Facile Synthesis of Nitrogen-Doped Graphene-Like Active Carbon Materials for High Performance Lithium-Sulfur Battery

MENG Quan-hua[1#], DENG Wen-wen[2#], LI Chang-ming[1,2,3*]

(1. *Institute for Clean Energy & Advanced Materials, School of Materials and Energy, Southwest University, Chongqing* 400715, *P.R. China*; 2. *Institute for Materials Science & Devices, School of Materials Science and Engineering, Suzhou University of Science & Technology, Suzhou* 215009, *P.R. China*; 3. *Institute for Advanced Cross-field Sciences, College of Life Science, Qingdao University, Qingdao* 266071, *P.R. China*)

Abstract: Lithium-sulphur (Li-S) battery is regarded as a promising energy storage device because of its high theoretical capacity. However, the low S utilization and short cycling life limit the commercial applications. In this work, nitrogen-doped graphene-like carbon (NGC) materials were synthesized by simply pyrolyzing and carbonizing the mixture of melamine ($C_3H_6N_6$) and L-cysteine ($C_3H_7NO_2S$). The graphene-like structure in NGC effectively buffered the volume change of S during the discharge/charge process and improved the cycling stability. Meanwhile, nitrogen-containing functional groups in NGC facilitated the transportation of ions and suppressed the dissolution of polysulphide (PS), enabling a high utilization of S. As expected, the NGC-8 (the mass ratio of melamine and L-cysteine being 8:1)/PS cathode delivered a high initial discharge capacity of 1164.1 mAh·g^{-1} at 0.2 C and still retained 909.4 mAh·g^{-1} capacity after 400 cycles with a slow capacity decay rate of 0.05% per cycle. Even at as high as 2 C, a high-rate capacity of 820 mAh·g^{-1} could be achieved.

Key words: lithium-sulphur battery; graphene-like carbon; volume change; cycling stability

CLC Number: O646 **Document Code:** A

With the increasing concerns on environmental and climatic problems, it becomes more and more important to develop next-generation of clean energy storage devices. The rechargeable lithium-sulfur (Li-S) battery with a ultrahigh theoretical specific capacity of 1675 mAh·g^{-1} and an energy density of 2567 Wh·kg^{-1} is regarded as one of the most promising candidates for next-generation of energy storage systems because of its low cost, natural abundance and non-toxicity of S[1-9]. However, there are still several issues which hinder its practical applications and further development including (a) the insulating nature of S and Li_2S_2/Li_2S limits the electron transport in the cathode, resulting in poor utilization of active materials; (b) large volume expansion (up to 80%) during charge/discharge cycles leads to pulverization of the electrode materials and reduces the cycling stability; (c) the dissolution of polysulfides (PS) during the charge/discharge process lowers coulombic efficiency and active material utilization; (d) The using of mental Li anode causes safety problems[4, 10-13]. Among these challenges, the shuttle effect caused by the dissolution of PS is the major one to cause poor performance of Li-S battery.

To solve the problems mentioned above, much effort has been made on design of various unique materials (carbon materials, conductive polymers, metal oxides/sulfides, and metal organic frameworks, et al.) to serve as the host of S[14-17], among which, graphene with excellent electrical conductivity, good mechanical extensibility, rational pore structure and adjustable specific surface area has attracted great research interest. Moreover, hetero-doping especially nitrogen (N)-doping can further improve the perfor-

Received: 2020-06-28, Revised: 2020-09-01 #. Equal contributors; * Corresponding author, Tel:(86-512)68096117, E-mail: ecmli@swu.edu.cn

mance of the graphene by enhancing conductivity and introducing more defects for high electrocatalytic activity[18]. Unfortunately, the complicated and expensive preparation process of graphene limits its practical application. Therefore, it is of great significance to design a facile and inexpensive method to prepare hetero-doped graphene-like carbon materials as the host of S.

In this work we prepared N-doped graphene-like carbon (NGC) materials by using the melamine and L-cysteine as precursors through less expensive and simple solid-state reaction, and studied their applications as the host of S cathode in Li-S battery. Results revealed that the graphene/PS composite—NGC-8/PS electrode exhibited a high specific capacity (1164.1 mAh·g^{-1} at 0.2 C) and a high rate capacity (820 mAh·g^{-1} at 2 C), as well as long cycle life (for 500 cycles with only 0.05% capacity decay rate per cycle). The excellent electrochemical performance was mainly ascribed to the graphene-like network structure and N-containing functional groups, which decreased the volume expansion of S and suppressed the shuttle effect during the discharge/charge process.

1 Experimental Details

1.1 Chemicals

All reagents including melamine ($C_3H_6N_6$, 99.99%), L-cysteine ($C_3H_7NO_2S$, 99.9%), sulfur (S) powder, lithium sulfide (Li_2S), lithium nitrate ($LiNO_3$), 1,2-dimethoxyethane (DME) and 1,3-dioxolane (DOL) were purchased from Sigma-Aldrich and directly used without any purification.

1.2 Syntheses of Nitrogen-Doped Graphene-Like Carbon Materials

The nitrogen-doped graphene-like carbon (NGC) was obtained through a classical method as reported previously. In a typical synthesis, a mixture of melamine (8 g) and L-cysteine (1 g) was firstly ground into a homogeneous powder for 10 h using a zirconia mortar, followed by a pyrolysis (600 ℃ for 3 h with a ramping rate of 5 ℃·min^{-1}) and carbonization (900 ℃ for 1.5 h with a ramping rate of 2 ℃·min^{-1}) process under argon atmosphere, thus the NGC-8 sample was obtained. Accordingly, NGC-4 and NGC-2 samples were prepared under the same experimental conditions with the mass ratios of melamine/L-cysteine=4:1 and 2:1 for NGC-4 and NGC-2, respectively.

1.3 Preparation of Li_2S_6 Polysulfide Catholyte

To prepare the soluble lithium polysulfide catholyte, 3.2 g of S powder and 0.94 g of Li_2S were added to 20 ml mixed liquid of DME and DOL with the volume ratio of 1:1 to render 6 mol·L^{-1} S in the form of Li_2S_6 in the solution. The obtained suspension was stirred at 60 ℃ for 12 h to yield the Li_2S_6 solution.

1.4 Fabrication of NGC/PS cathode

NGC, carbon nanotube (CNT) and polyvinylidenefuoride (PVDF) binder were homogeneously mixed with the mass ratio of 8:1:1 in a N-methyl-2-pyrrolidone solvent to form a slurry. Then the slurry was uniformly coated on the carbon paper, and followed by drying at 80 ℃ in an oven to obtain NGC cathode film. Subsequently, an appropriate amount of Li_2S_6 catholyte was dropped on the NGC film as the active material to form NGC/PS cathode. The mass of active material S was controlled by about 1.9 mg·cm^{-2} in each electrode.

1.5 Battery Assembly and Electrochemical Measurements

The CR2032-type coin cells consisting of the NGC/PS cathode, Celgard separator and Li metal anode were assembled in an argon-filled glovebox. The electrolyte was composed of 1 mol·L^{-1} LiTFSI and 0.2 mol·L^{-1} $LiNO_3$ dissolved in the DME and DOL (1:1 vol) solution. The galvanostatic charge-discharge tests were conducted at different current densities between 1.7 V and 2.7 V using a LAND galvanostatic charge-discharge instrument. CV tests (scanning from 1.7 V to 2.7 V) and EIS measurements (the frequency range from 0.01 Hz to 10 kHz) were performed using CHI-760 electrochemical workstation. All the cells were tested at room temperature.

2 Results and Discussion

The melamine was firstly polymerized at 600 ℃ to form L-cysteine decorated C_3N_4 nanosheets with the help of the high reactivity of thiol group on the

L-cysteine. Subsequently, it was carbonized at 900 ºC to obtain the NGC samples. Fig. 1 shows the typical images of the as-prepared samples observed by field emission scanning electron microscope (FE-SEM) and transmission electron microscope (TEM). All the NGC-8, NGC-4 and NGC-2 samples displayed the 3D interconnected nanostructure. Differently, the NGC-8 sample (Fig. 1 G-I) exhibited a better interconnected structure in comparison with NGC-4 (Fig. 1 D-F) and NGC-2 (Fig. 1 A-C), which is more beneficial to the electrolyte permeation, guaranteeing a higher capacity. In addition, the corresponding elemental mapping images (Fig. 1 and Fig. S1 in the Supporting Information) indicate that C, O and N were uniformly distributed in the NGC materials.

X-ray diffraction (XRD) and Raman analyses were conducted to identify the phase structure and crystallinity of the samples. As shown in Fig. 2A, all the samples exhibited a broad diffraction peak at around 26º corresponding to the (002) plane of carbonaceous materials[19]. Fig. 2B shows the Raman patterns of NGC. It is well known that the two characteristic peaks of the samples at 1330 cm^{-1} (D band) and 1585 cm^{-1} (G band) are associated with the defective carbon and graphitic carbon, respectively[20]. It can be found that the intensity ratio (I_D/I_G) of D band and G band is about 1.51 for NGC-8 (Tab. S1), which is larger than those of NGC-4 (I_D/I_G=1.37) and NGC-2 (I_D/I_G=1.28), indicating that NGC-8 owns a more disordered structure owing to the massive addition of melamine[21]. Additionally, the nitrogen adsorption-desorption isotherms measurements were performed to investigate the pore structure of the samples. The measured Brunauer-Emmett-Teller (BET) surface ar-

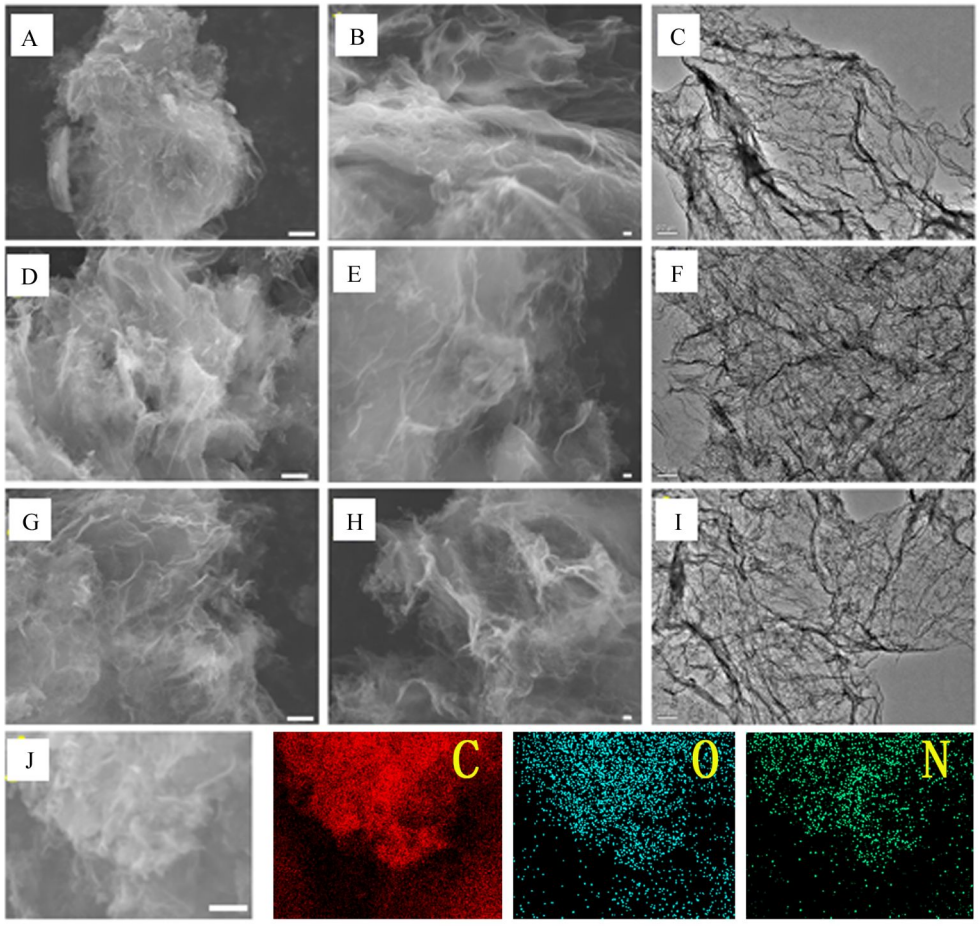

Fig. 1 FE-SEM and TEM images. (A, B, C) NGC-8, (D, E, F) NGC-4 and (G, H, I) NGC-2, and (J) Elemental mapping images of NGC-8. Scale bars, (A, D, G and J) 1 μm; (B, E and H) 100 nm; (C, F, and I) 0.2 μm.

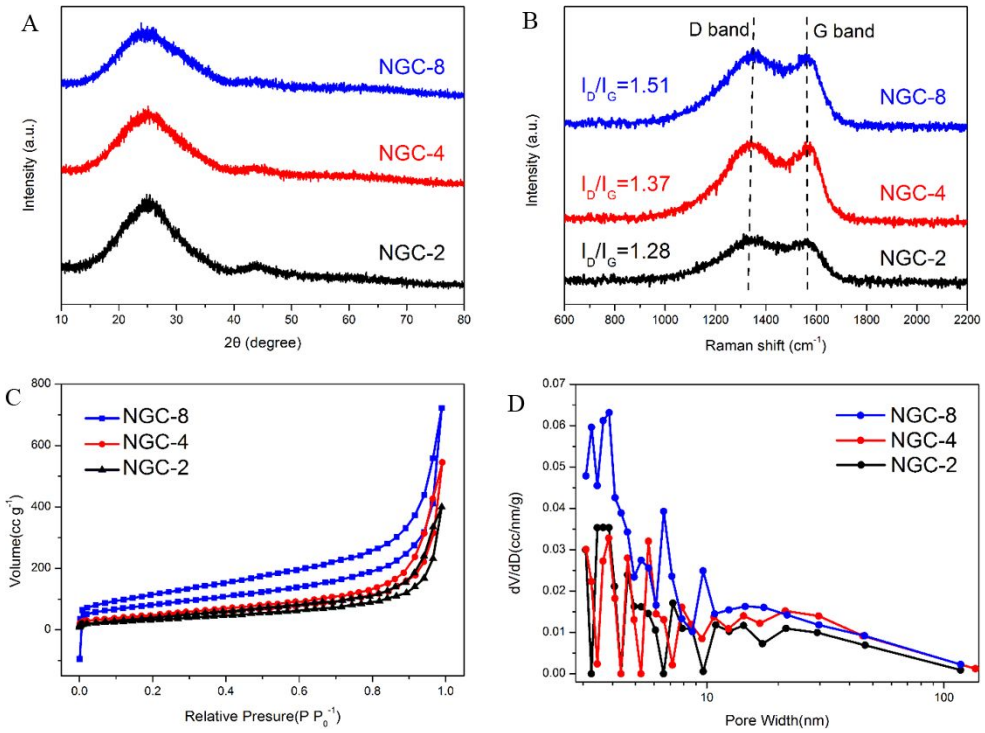

Fig. 2 (A) XRD patterns, (B) Raman spectra, (C) N_2 adsorption and desorption isotherms and (D) the corresponding pore size distribution curves of the NGC samples.

eas of the NGC-8, NGC-4 and NGC-2 were 304, 161 and 130 $m^2 \cdot g^{-1}$, respectively. The pore size distribution (Fig. 2D) of the samples based on Barrett-Joyner-Halenda (BJH) calculations indicts the existence of abundant mesopores with the sizes ranged from 3 to 50 nm. Furthermore, the pore volume calculated from the N_2 sorption isotherms was 1.016 $cm^{-3} \cdot g^{-1}$ for NGC-8, significantly larger than those of NGC-4 (0.827 $cm^{-3} \cdot g^{-1}$) and NGC-2 (0.604 $cm^{-3} \cdot g^{-1}$), accelerating the transportation of Li^+ (Tab. S1).

The surface chemical compositions and elemental states of the products were studied by X-ray photoelectron spectroscope (XPS) and Fourier transform infrared (FT-IR) spectroscope. The XPS survey spectra (Fig. 3A) clearly reveal that all the materials consisted of C, N, and O, which are well in accord with the SEM mapping results (Fig. 1). The characteristic peak in the FT-IR spectra (Fig. 3B) located at around 1700 cm^{-1} is ascribed to the symmetric stretching vibrations of C=O, C=N and COO- groups. Meanwhile, the broad peak at around 1230 cm^{-1} is related to the vibrations of C-OH, C-O-C and aromatic C-N groups[22-24]. Moreover, The IR band related to the O-H stretching vibrations at 3450 cm^{-1} is observed for all the samples, indicating the existence of surface hydroxylic groups and chemisorbed water[25]. All these IR features indicate that most functional groups were kept in NGC after carbonization, which might make contributions to the interaction between NCG and S or lithium polysulfide.

The high resolution C1s XPS spectra of all the NGC samples can be deconvoluted into five peaks which correspond to C=C (284.47 eV), C-C (284.9 eV), C=N/C-O (285.6 eV), C=O/C-N (286.6) and -COO (288.9 eV) (Figure 4A, D, and G)[26]. Apparently, as the mass ratio of melamine and L-cysteine increases, the intensity of C=C gradually diminishes and finally disappears for NGC-8, implying its more disordered structure, which is consistent with the result of I_D/I_G. As shown in Fig. 4B, E and H, nitrogen in the samples mainly exists in the forms of pyridinic (398 eV), pyrrolic (398.8 eV), quaternary (400.8 eV) and oxidized (402.9 eV) nitrogen (Table S2), among which, the former three types of N account for major part[27].

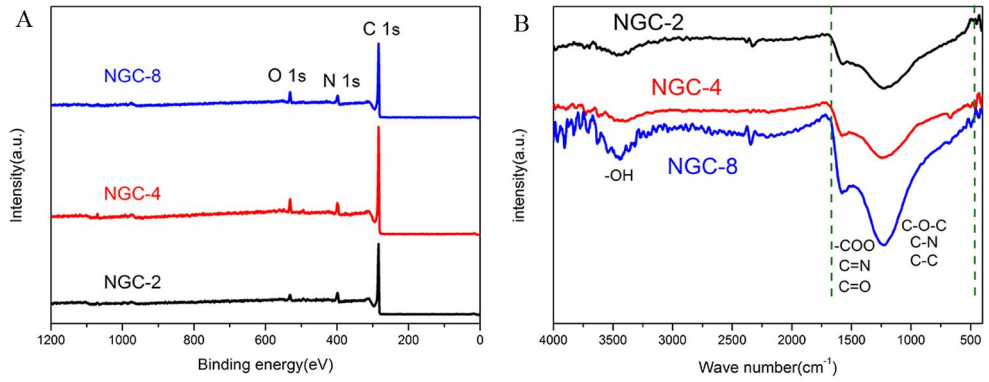

Fig. 3 (A) XPS survey spectra and (B) FTIR spectra of the NGC samples.

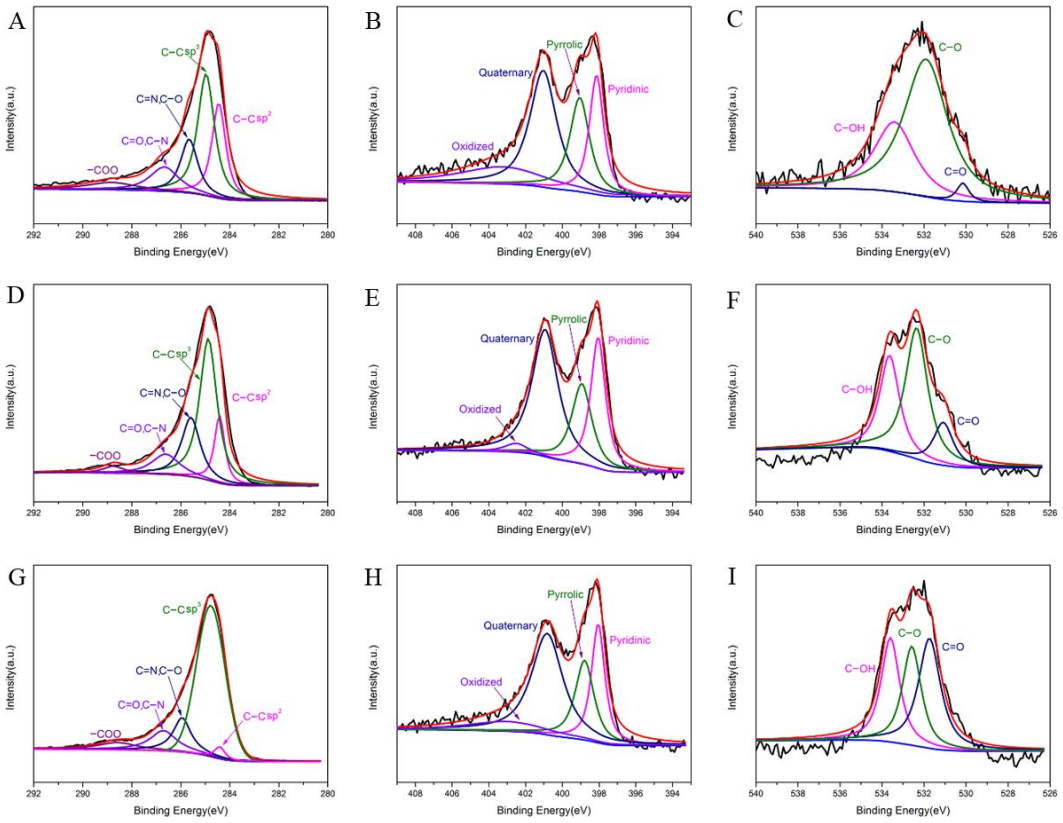

Fig. 4 High resolution XPS spectra. (A) C 1s, (B) N 1s, (C) O 1s of NGC-2; (D) C 1s, (E) N 1s, (F) O 1s of NGC-4; (G) C 1s, (H) N 1s, (I) O 1s of NGC-8.

The content for these three types of N in each GNC sample is as high as 8%~10%, which is beneficial to substantial chemisorption of lithium polysulfides[28]. Normally, pyridinic N and pyrrolic N have higher binding energies than lithium polysulfides, and can enhance the absorption of lithium polysulfides. Quaternary N has a relatively low binding energy as compared to lithium polysulfides, but can improve the lithium ion (Li^+) binding affinity in lithium polysulfides[29]. From Table S2, one can conclude that quaternary N is of the highest content in comparison with the other two forms of N, indicating that the interaction between Li and N seems dominant due to the high binding affinity in lithium polysulfides. Meanwhile, it can be found that the exiting forms of O in NGC are C=O (531.7 eV), C-O (532.5 eV) and C-OH

(533.6 eV)(Tab. S3)[30].

To evaluate the electrochemical performance of NGC in Li-S battery, the NGC-8 films with an appropriate amount of Li_2S_6 polysulfide catholyte were used as the cathode. The cyclic voltammetry (CV) measurement was conducted at a scan rate of 0.1 mV·s^{-1} in the voltage range of 1.7 to 2.7 V versus Li/Li^+ after the rate testing. As shown in Figure 5A and Fig. S2, there are two main reduction peaks at about 2.28 V and 2.01 V during the cathodic scan, which are related to the open ring reaction of S_8 to long chain polysulfides (Li_2S_x $4 < x < 8$) and the conversion of these long chain polysulfides to Li_2S_2/Li_2S, respectively[31-32]. Similarly, there are also one sharp peak at 2.36 V and a shoulder peak at 2.42 V in the subsequent anodic scan, involving the formation of Li_2S_x ($4 < x < 8$) and the continued oxidation of lithium polysulfide to elemental sulfur, respectively[33-35]. It is worth noting that the NGC-8 cathode exhibits stronger and more lapped redox peaks than the NGC-4 and NGC-2 cathodes (Fig. S2), indicating its higher specific capacity and long cycling life. Moreover, the CV curves almost show no obviously change and position shift, indicating the high electrochemical reversibility and good stability of the NGC/PS cathode.

The rate capability test was conducted at different rates and the results are shown in Fig. 5C. At the current densities of 0.2, 0.5, 1 and 2 C (1 C = 1675 mA·g^{-1}), the NGC-8 exhibited the reversible specific capacities of 1280, 1130, 990, and 820 mAh·g^{-1}, respectively, which are higher than those of NGC-4 and NGC-2. More importantly, when the rate was gradually reduced to 0.2 C, a high capacity of 1200 mAh·g^{-1} could still be obtained for NGC-8/PS. The excellent rate capacity of the NGC-8/PS cathode was mainly attributed to its unique 3D interconnected porous nanostructure and adequate N-containing functional groups, which could effectively buffer the volume expansion and depress the shuttle effect during the cycling process[36-40]. To investigate the cyclic stability, the galvanostatic charge/discharge curves of the NGC/PS cathodes were measured at the current density of 0.2 C. After the activation at 0.05 C for one

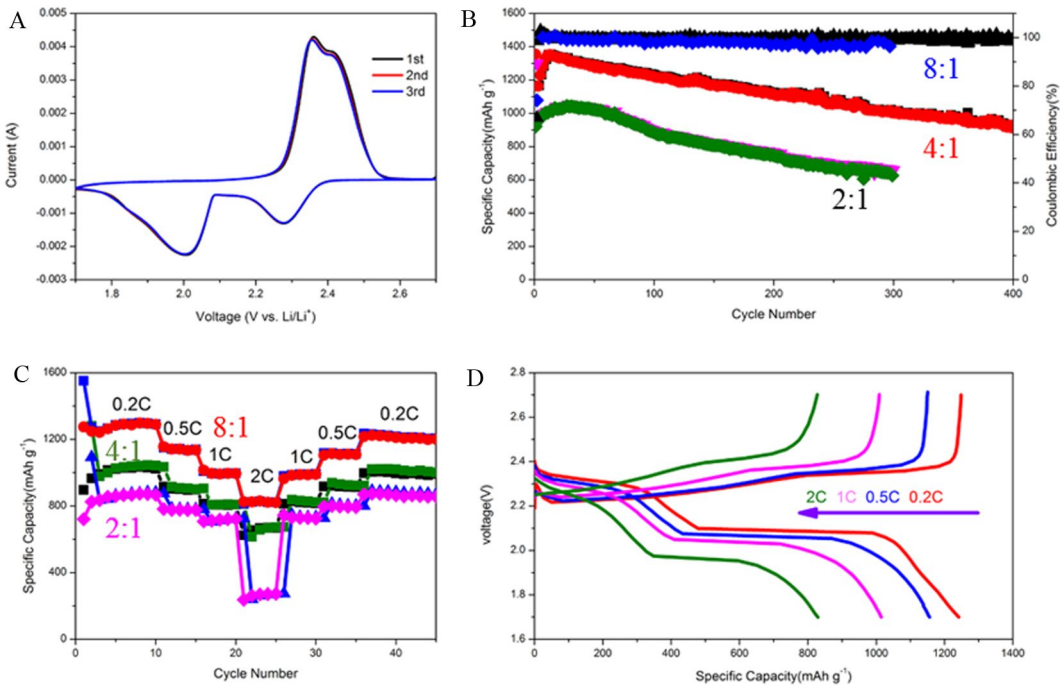

Fig. 5 Electrochemical performance of the as-prepared NGC/PS. (A) CV curves of NGC-8; (B) Cycling performance curves of NGC-2, NGC-4, and NGC-8 at a current rate of 0.2 C; (C) rate capabilities; (D) galvanostatic discharge/charge curves of NGC-8 at different rates from 0.2 C to 2 C.

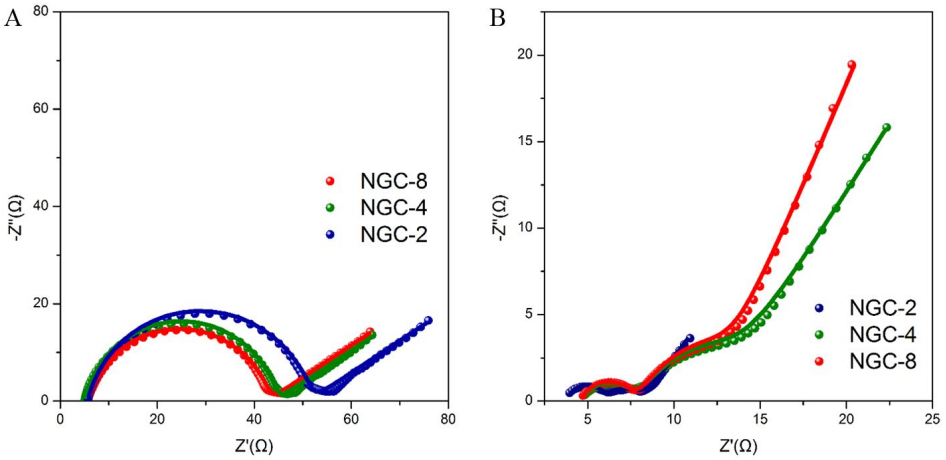

Fig. 6 Nyquist plots of the cells before cycling (A) and after 50 cycles (B).

cycle, the initial discharge capacity (calculated based on the weight of S) of NGC-8/PS, NGC-4/PS and NGC-2/PS were 1164, 962.4 and 823.6 mAh·g^{-1} at 0.2 C, respectively (Fig. 5B).

The excellent electrochemical performance of the NGC/PS cathodes was investigated by electrochemical impedance spectroscopy (EIS), and the results are shown in Fig. 6 and Tab. S2. As shown in Fig. 6A, all the Nyquist plots show a semicircle in the high frequency region and a slope line in the low frequency region before cycling, which can be ascribed to the charge-transfer resistance and the ion diffusion process, respectively. Apparently, after 50 cycles, there are two semicircles appeared in the high frequency region (Fig. 6B). The right one is related to the surface layer resistance (R_{sf}) between soluble polysulfides and electrode, and the other one represents the charge-transfer resistance (R_{ct})[41]. The detailed fitting values obtained by the equivalent circuits are displayed in Tab. S4. It can be noted that the NGC-8/PS electrode exhibited a smaller value of R_{ct} (36.9 Ω) than NGC-4/PS (39.2 Ω) and NGC-2/PS (45.6 Ω), indicating the better reaction kinetics for NGC-8/PS.

To explain the excellent cycling stability of NGC/PS reasonably, after 500 cycles at 1 C, the batteries were disassembled and analyzed by SEM (Fig. S3). It can be seen that compared with NGC-4/PS and NGC-2/PS, the NGC-8/PS electrode maintained a

Tab. 1 Performance comparison of NGC-8/PS with the sulfur host carbon materials reported previously.

Cathode	Current density	Sulfur loading/ (mg·cm^{-2})	Cycle	Capacity/ (mAh·g^{-1})	Reference
S-NPC/G	1 C	2.4	300	608	[40]
3DP-FDE	0.2 C	3	200	752	[41]
WSAC-8/S	1 C	1	200	800	[42]
rGO/PC/S	1 C	1.2	300	848	[43]
a-NOSPC/S	0.5 C	1.1	400	740	[44]
S-GO/MWCNT	0.2 C	1.5-2	400	670	[45]
rNGO/S	1 C	1.2	200	592	[46]
S/NDPC-1	1 C	1	500	541	[47]
NGC-8/PS	0.2 C	2	400	910	This work
	1 C	2	500	800	

more complete structure, further implying that NGC-8 can effectively alleviate the volume expansion during discharge/charge process. In addition, as can be seen in Tab. 1, the NGC-8/PS electrode exhibited more excellent electrochemical behavior in comparison with those of previously reported carbon materials[35-40], indicating its great potential in the practical application.

3 Conclusions

In summary, the N-doped graphene-like carbon materials were successfully prepared by a low-cost, simple solid-state reaction, and were further used as a host material for S. When using as the cathode in Li-S battery, the NGC-8/PS electrode exhibited a high specific capacity of 909.4 mAh·g^{-1} for 400 cycles at 0.2 C, a high rate capacity of 820 mAh·g^{-1} at 2 C and excellent cycling stability with a small capacity decay rate of 0.05% per cycle over 500 cycles. The excellent battery performance was ascribed to the following reasons: (a) The graphene-like network structure facilitateed electrolyte penetration, and offered pathways for rapid transfer of electron and fast mass transport of lithium ions; (b) the abundant N-containing functional groups were strongly bound to polysulfide, thus effectively suppressing the shuttle effect. The feasible and inexpensive preparation method together with the outstanding electrochemical performance may hold great promise for the potential applications of NGC materials in high-performance Li-S battery.

Supporting Information

Additional experimental details. This material is available free of charge via the Internet at http://electrochem.xmu.edu.cn.

Acknowledgements

This work is particularly dedicated to memory of Professor Chuan-sin Cha for his pass away on Aug. 1 of 2019. Professor Cha was internationally well-known electrochemist and one of the founders of Electrochemistry in China. It will take a long time for us coming to grips with this loss. He was the dear supervisor for Changming's MS and PhD programs in Wuhan University. He will be remembered for his profound knowledge, remarkable practice and invaluable advices to guide us in electrochemistry research for years. He will be remembered as an extremely creative and thoughtful professor for his prominent contributions to electrochemistry, being able to seamlessly combine his profound background in electrochemistry passionately with industrialization of his innovations in green energy systems. He had trained many outstanding students becoming accomplished scientists in China and world. Inspiring his spirit "Coming with a heart, leaving with nothing", we are certain that we will follow his way to devote our life to sciences advances.

This work was supported by the National Natural Science Foundation of China (No. 21905194), the Natural Science Foundation of Jiangsu Province (No. SBK2018042005), the Natural Science Foundation of the Jiangsu Higher Education Institution of China (Grant No. 18KJB150029).

References:

[1] Yang Y, Zheng G Y, Cui Y. Nanostructured sulfur cathodes[J]. Chemical Society Reviews, 2013, 42(7): 3018-3032.

[2] Manthiram A, Chung S H, Zu C X. Lithium-sulfur batteries: Progress and prospects[J]. Advanced Materials, 2015, 27(12): 1980-2006.

[3] Rosenman A, Markevich E, Salitra G, et al. Review on Li-sulfur battery systems: an integral perspective[J]. Advanced Energy Materials, 2015, 5(16): 1500212.

[4] Evers S, Nazar L F. New approaches for high energy density lithium-sulfur battery cathodes[J]. Accounts of Chemical Research, 2013, 46(5): 1135-1143.

[5] Pope M A, Aksay I A. Structural design of cathodes for Li-S batteries[J]. Advanced Energy Materials, 2015, 5(16): 1500124.

[6] Wang J L, He Y S, Yang J. Sulfur-based composite cathode materials for high-energy rechargeable lithium batteries[J]. Advanced Materials, 2015, 27(3): 569-575.

[7] Bruce P G, Freunberger S A, Hardwick L J, et al. Li-O_2 and Li-S batteries with high energy storage[J]. Nature Materials, 2012, 11(1): 19-29.

[8] L. Ma, Zhuang H L L, Wei S Y, et al. Enhanced Li-S batteries using amine-functionalized carbon nanotubes in the cathode[J]. ACS Nano, 2016, 10(1): 1050-1059.

[9] Fang R P, Zhao S Y, Hou P X, et al. 3D interconnected electrode materials with ultrahigh areal sulfur loading for Li-S batteries[J]. Advanced Materials, 2016, 28(17): 3374-

3382.

[10] Ji X L, Lee K T, Nazar L F. A highly ordered nanostructured carbon-sulphur cathode for lithium-sulphur batteries[J]. Nature Materials, 2009, 8(6): 500-506.

[11] Ji L W, Rao M M, Aloni S, et al. Porous carbon nanofiber-sulfur composite electrodes for lithium/sulfur cells[J]. Energy & Environmental Science, 2011, 4(12): 5053-5059.

[12] Yao H B, Zheng G Y, Hsu P C, et al. Improving lithium-sulphur batteries through spatial control of sulphur species deposition on a hybrid electrode surface[J]. Nature Communications, 2014, 5: 3943.

[13] Tao X Y, Wang J G, Liu C, et al. Balancing surface adsorption and diffusion of lithium-polysulfides on nonconductive oxides for lithium-sulfur battery design[J]. Nature Communications, 2016, 7: 11203.

[14] Ye H, Yin Y X, Xin S, et al. Tuning the porous structure of carbon hosts for loading sulfur toward long lifespan cathode materials for Li-S batteries[J]. Journal of Materials Chemistry A, 2013, 1(22): 6602-6608.

[15] Puthirath A B, Baburaj A, Kato K, et al. High sulfur content multifunctional conducting polymer composite electrodes for stable Li-S battery[J]. Electrochimica Acta, 2019, 306: 489-497.

[16] Liu X, Huan J Q, Zhang Q, et al. Nanostructured metal oxides and sulfides for lithium-sulfur batteries[J]. Advanced Materials, 2017, 29(20): 1601759.

[17] Yilmaz G, Peh S B, Zhao D, et al. Atomic- and molecular-level design of functional metal-organic frameworks (MOFs) and derivatives for energy and environmental applications[J]. Advanced Science, 2019, 6(21): 1901129.

[18] Yang H B, Miao J W, Hung S F, et al. Identification of catalytic sites for oxygen reduction and oxygen evolution in N-doped graphene materials: Development of highly efficient metal-free bifunctional electrocatalyst[J]. Science Advance, 2016, 2(4): e1501122.

[19] Song J X, Xu T, Gordin M L, et al. Nitrogen-doped mesoporous carbon promoted chemical adsorption of sulfur and fabrication of high-areal-capacity sulfur cathode with exceptional cycling stability for lithium-sulfur batteries[J]. Advanced Functional Materials, 2014, 24(9): 1243-1250.

[20] Zhou G M, Wang D W, Yin L C, et al. Oxygen bridges between NiO nanosheets and graphene for improvement of lithium storage[J]. ACS Nano, 2012, 6(4): 3214-3223.

[21] Guo J C, Xu Y H, Wang C S. Sulfur-impregnated disordered carbon nanotubes cathode for lithium-sulfur batteries[J]. Nano Letters, 2011, 11(10): 4288-4294.

[22] Liu J H, Li W F, Duan L M, et al. A graphene-like oxygenated carbon nitride material for improved cycle-life lithium/sulfur batteries[J]. Nano Letters, 2015, 15(8): 5137-5142.

[23] Park S, Lee K S, Bozoklu G, et al. Graphene oxide papers modified by divalent ions—enhancing mechanical properties via chemical cross-linking[J]. ACS Nano, 2008, 2(3): 572-578.

[24] Shen W Z, Ren L W, Zhou H, et al. Facile one-pot synthesis of bimodal mesoporous carbon nitride and its function as a lipase immobilization support[J]. Journal of Materials Chemistry, 2011, 21(11): 3890-3894.

[25] Biniak S, Szymański G, Siedlewski J, et al. The characterization of activated carbons with oxygen and nitrogen surface groups[J]. Carbon, 1997, 35(12): 1799-1810.

[26] Yang H B, Miao J W, Hung S F, et al. Identification of catalytic sites for oxygen reduction and oxygen evolution in N-doped graphene materials: Development of highly efficient metal-free bifunctional electrocatalyst[J]. Science Advances, 2016, 2(4): e1501122.

[27] Chen C, Xu G B, Wei X L. A macroscopic three-dimensional tetrapod-separated graphene-like oxygenated N-doped carbon nanosheet architecture for use in supercapacitors[J]. Journal of Materials Chemistry A, 2016, 4(25): 9900-9909.

[28] Pei F, Lin L L, Fu A, et al. A two-dimensional porous carbon-modified separator for high-energy-density Li-S batteries[J]. Joule, 2017, 2(2): 323-336.

[29] Zhu L, Jiang H T, Ran W X, et al. Turning biomass waste to a valuable nitrogen and boron dual-doped carbon aerogel for high performance lithium-sulfur batteries[J]. Applied Surface Science, 2019, 489: 154-164.

[30] Liu J H, Li W F, Duan L M, et al. A graphene-like oxygenated carbon nitride material for improved cycle-life lithium/sulfur batteries[J]. Nano Letters, 2015, 15(8): 5137-5142.

[31] Yamin H, Gorenshtein A, Penciner J, et al. Oxidation/reduction mechanismsof polysulfidesin THF solutions[J]. Journal of Electrochemstry Society, 1988, 135(5): 1045-1048.

[32] Elazari R, Salitra G, Garsuch A, et al. Sulfur-impregnated activated carbon fiber cloth as a binder-free cathode for rechargeable Li-S batteries[J]. Advanced Materials, 2011, 23(47): 5641-5644.

[33] Akridge J R, Mikhaylik Y V, White N. Li/S fundamental chemistry and application to high-performance rechargeable batteries[J]. Solid State Ionics, 2004, 175(1/4): 243-245.

[34] Nelson J, Misra S, Yang Y. et al. *In operando* X-ray diffraction and transmission X-ray microscopy of lithium

sulfur batteries[J]. Journal of the American Chemical Society, 2012, 134(14): 6337-6343.

[35] Jayaprakash N, Shen J, Moganty S S, et al. Porous hollow carbon@sulfur composites for high-power lithium-sulfur batteries[J]. Angewandte Chemie International Edition, 2011, 50(26): 5904-5908.

[36] Cai J J, Wu C, Zhu Y, et al. Sulfur impregnated N, P co-doped hierarchical porous carbon as cathode for high performance Li-S batteries[J]. Journal of Power Sources, 2017, 341: 165-174.

[37] Tripathi A K, Verma Y L, Singh R K. Thermal, electrical and structural studies on ionic liquid confined in ordered mesoporous MCM-41[J]. Journal of Materials Chemistry A, 2015, 3(47): 23809-23820.

[38] Pei F, An T H, Zang J, et al. From hollow carbon spheres to N-doped hollow porous carbon bowls: rational design of hollow carbon host for Li-S batteries[J]. Advanced Energy Materials, 2016, 6(8): 1502539.

[39] Zheng Z M, Guo H C, Pei F, et al. High sulfur loading in hierarchical porous carbon rods constructed by vertically oriented porous graphene-like nanosheets for Li-S batteries[J]. Advanced Functional Materials. 2016, 26(48): 8952-8959.

[40] Chen K, Sun Z H, Fang R P, et al. Metal-organic frameworks (MOFs)-derived nitrogen-doped porous carbon anchored on graphene with multifunctional effects for lithium-sulfur batteries[J]. Advanced Functional Materials, 2018, 28(38): 1707592.

[41] Gao X J, Sun Q, Yang X F, et al. Toward a remarkable Li-S battery via 3D printing[J]. Nano Energy, 2019, 56: 595-603.

[42] Wu P, Chen L H, Xiao S S, et al. Insight into the positive effect of porous hierarchy in S/C cathodes on the electrochemical performance of Li-S batteries[J]. Nanoscale, 2018, 10(25): 11861-11868.

[43] Zhang H, Gao Q M, Qian W W, et al. Binary hierarchical porous graphene/pyrolytic carbon nanocomposite matrix loaded with sulfur as a high-performance Li-S battery cathode[J]. ACS Applied Materials & Interfaces, 2018, 10 (22): 18726-18733.

[44] Zhong M E, Guan J D, Sun J C, et al. Carbon nanodot-decorated alveolate N, O, S tridoped hierarchical porous carbon as efficient electrocatalysis of polysulfide conversion for lithium-sulfur batteries[J]. Electrochimica Acta, 2019, 299: 600-609.

[45] Kim J, Kang Y, Song S W, et al. Freestanding sulfur-graphene oxide/carbon composite paper as a stable cath ode for high performance lithium-sulfur batteries[J]. Electrochimica Acta, 2019, 299: 27-33.

[46] Duan L F, Zhao L J, Cong H, et al. Plasma treatment for nitrogen-doped 3D graphene framework by a conductive matrix with sulfur for high-performance Li-S batteries[J]. Small, 2019, 15(7): 1804347.

[47] Wang S X, Zou K X, Qian Y X, et al. Insight to the synergistic effect of N-doping level and pore structure on improving the electrochemical performance of sulfur/N-doped porous carbon cathode for Li-S batteries[J]. Carbon, 2019, 144: 745-755.

类石墨烯类活性炭材料的简易合成及其在锂硫电池中的应用研究

孟全华[1#],邓雯雯[2#],李长明[1,2,3*]

(1. 西南大学材料与能源学院,洁净能源和先进材料研究所,重庆 400715; 2. 苏州科技大学材料科学与工程学院,江苏 苏州 215009; 3. 青岛大学生命科学学院,先进跨学科科学研究所,山东 青岛,266071)

摘要: 锂硫电池由于具有较高的理论容量被视为一种最具发展潜力的储能装置. 然而, 硫的利用率较低及循环寿命短等问题限制着其商业化进程. 本文通过一种简单易行的方法将三聚氰胺($C_3H_6N_6$)和 L 半胱氨酸($C_3H_7NO_2S$)碳化,制备出一种氮掺杂类石墨烯活性碳材料(NGC). 该材料的类石墨烯结构能够有效抑制锂硫电池在充放电过程中产生的体积效应,以此提升其循环性能. 不仅如此,材料中含有的含氮官能团还可以促进离子转移,抑制多硫化物的溶解,进而提升硫的利用率. 其中,制备出的 NGC-8/PS 复合电极用于锂硫电池时在 0.2 C 的电流密度下初始容量为 1164.1 mAh·g^{-1}, 在经过 400 圈的充放电循环之后依然具有 909.4 mAh·g^{-1} 的比容量,每圈容量衰减仅为 0.05%,甚至在 2C 的电流密度下也能达到 820 mAh·g^{-1} 的高比容量.

关键词: 锂硫电池;类石墨烯碳材料;体积效应;循环稳定性